

## SUPERCritical WATER CONVECTION LOOP (NSC KIPT) FOR MATERIALS ASSESSMENT FOR THE NEXT GENERATION REACTORS

A.S. Bakai<sup>1</sup>, V.N. Boriskin<sup>1</sup>, A.N. Dovbnya<sup>1</sup>, S.V. Dyuldy<sup>1</sup> and D.A. Guzonas<sup>2</sup>

<sup>1</sup> National Science Center “Kharkiv Institute of Physics and Technology”, Kharkiv, Ukraine

<sup>2</sup> AECL, Chalk River Laboratories, Chalk River, Ontario, Canada

### Abstract

The current status of the development of the KIPT sited Canada-Ukraine Electron Irradiation Test Facility, integrating the specially designed Supercritical Water Convection Loop with an irradiation chamber coupled to a 10 MeV, 10 kW LPE-10 linac, is described with special attention paid to the methodology of future simulation experiments and the results of computer modeling of thermal-hydraulic and irradiation specific parameters of the facility.

### 1. Introduction

The Supercritical Water-Cooled Reactor (SCWR) is one of the most promising nuclear technologies identified for R&D under the Generation IV (GenIV) program [1]. At Atomic Energy of Canada Limited (AECL) the SCWR has been recognized as the next evolutionary step of CANDU technology and given a high priority status [2]. Along with the Very High-Temperature Reactor (VHTR) and Molten Salt Reactor (MSR) systems, SCWR technologies (either CANDU or Super-WWER related) may also be considered as possible candidates for GenIV prospects for the nuclear power industry of Ukraine.

The lack of reliable design-relevant data on the properties of structural materials exposed to neutron irradiation under a pressure of supercritical water (SCW) coolant of about 25 MPa and temperatures ranging from 350°C (core inlet) to 625°C (core outlet) are major factors limiting our ability to assess the practicality of an SCWR. Very different construction materials are being considered as candidates for the SCWR; austenitic and ferritic-martensitic (F/M) stainless steels (SS), Ni-, Zr- and Ti-based alloys, as well as innovative oxide dispersion strengthened (ODS) steels and alloys. Their corrosion rates and stress corrosion cracking (SCC) susceptibility in pure SCW is being studied experimentally using SCW convection loops (SCWCL) without irradiation (a survey of current R&D can be found, *e.g.*, in ref. 3).

This experience is insufficient, however, for the design and construction of the SCWR since irradiation effects are known to affect the corrosion behaviour of materials. Currently there are no experimental data on the corrosion and SCC of structural materials in flowing SCW under irradiation (the sparse data available [3] are limited to experiments with pre-irradiated samples). In general, the properties of materials in contact with SCW coolant in a radiation field have not been investigated in detail. Materials behaviour in laminar and turbulent SCW flows under irradiation have not been described in the accessible literature. The irradiation-induced effects of SCW radiolysis on flow control and instabilities, *incl.* transitions from the subcritical to supercritical state, are of great interest for SCWR development, and can also influence the corrosion of structural materials. These issues require thorough studies using dedicated experimental facilities that provide simultaneous exposure of samples to both SCW and irradiation.

In 2009, the Canadian government provided funding to support collaborative activities between the NSC Kharkiv Institute of Physics and Technology (KIPT) and their colleagues from AECL's Chalk River Laboratories aimed at the development of advanced experimental facilities and methodologies for the assessment of putative structural materials for SCW reactors. The advanced skills of KIPT experts in structural material design and testing, along with their experience in simulation of reactor in-pile irradiation using gamma, electron and ion irradiation, will be employed for candidate materials assessment. These activities are managed by the Science & Technology Centre in Ukraine (STCU) within the framework of the Canada-Ukraine partner project STCU-P4841 "SCW convection loop for materials assessment for the next generation reactors". The Project goal is the design and construction of the Canada-Ukraine Electron Irradiation Test Facility (CU-EITF), having a specially developed SCWCL with a target test cell subjected to electron irradiation. After commissioning, the CU-EITF will be used for collaborative tests of structural materials for GenIII+ and GenIV reactors of the CANDU family. The objective of this correspondence is to report on the current state of the facility and first results of the Project.

## 2. Methodology

The methodology of the CU-EITF experimental program is based on long-standing KIPT experience with simulation studies of reactor irradiation effects in materials by means of ( $e^-$ ,  $\gamma$ ) and/or ion beams produced by particle accelerators. More than 25 electron [4], ion and plasma accelerators of different types are operating in KIPT, and some new accelerators are under construction [5]. Irradiations are followed by structural, corrosion and mechanical tests of irradiated materials.

As compared to direct in-pile reactor tests of materials, the key benefits of simulation experiments are lower cost, shorter set-up and irradiation time, greater control of irradiation environment parameters (temperature, fluence, dose, etc.), and the possibility of investigating irradiated samples outside of hot cells due to the negligible activation of materials. These features are very attractive, *esp.* at early stages of reactor material development. On the other hand, the difference of radiation fields in reactors and in simulation facilities must be taken into account when making conclusions on the suitability of materials for use in targeted nuclear reactors. It requires developments of scaling models and advanced computer simulation of irradiation environments of both systems under consideration.

Recently [6–8] this approach of simulation studies has been applied to the evaluation of irradiation effects on the corrosion of Hastelloy™ type Ni-Mo alloys, promising structural materials for the GenIV MSR, exposed to 700 hrs long irradiation by 10 MeV electron beam (EB) in a melt of fluoride salts at 660°C. The study was carried out at the KIPT-sited EITF using the LPE-10 electron linac and a specially designed target container assembly [6]. Rapid post-irradiation tests revealed considerable enhancement of molten salt induced corrosion rates of irradiated specimens as compared to those of unirradiated reference samples [6,7]. The irradiation effect has been attributed to microstructural and compositional changes [7] of the alloys and characterized quantitatively by observed corrosion rates correlated to detailed computational dosimetry of EB energy deposition and radiation damage of specimens. The scalability of the EITF experiment to the target MSR ( $n$ ,  $\gamma$ ) irradiation environment has been studied [8] by means of Monte Carlo simulation of EITF EB irradiation and MSR neutronics. Though the bulk radiation damage rate was found to be much smaller for EB irradiation, it has been shown that the KIPT EITF is capable of reproducing of the MSR (as well as SCWR) relevant range of the specific energy deposition of radiation, the major physical param-

ter that controls the irradiation effects on material behaviour at the interface with the corrosion medium.

A similar experimental/computational approach is being taken for the further extension of the EITF to the SCWR-relevant CU-EITF program. The facility design and construction, the planning of simulation experiments and the developments of advanced computer models are being carried out in parallel from the very early stages of the Project. But it should be emphasised that the principal advance in the projected CU-EITF vs. the operating EITF is the incorporation of the dynamic circulation of the corrosion medium (SCW) compared to the static setup of the MSR-related experiment that used sealed target ampoules filled with molten fluorides. It is achieved by the combination of a target irradiation cell with a water circulation loop that can operate both in subcritical and supercritical modes. Consequently, it requires additional effort to predict the interplay of EB irradiation with the hydrodynamics of SCW flow and the thermal hydraulic parameters of the facility.

### 3. CU-EITF design overview

A schematic of the major components of the CU-EITF design is shown in Figure 1. It is conceptually similar to various currently operating and developing SCW natural and forced circulation loops (see, e.g., [9,10]) but differs notably by the incorporation of the electron linac LPE-10 and the corresponding irradiation cell (a target). The dimensions of the target loop and additional components are determined by the size and arrangement of the KIPT facility housing the electron accelerator.

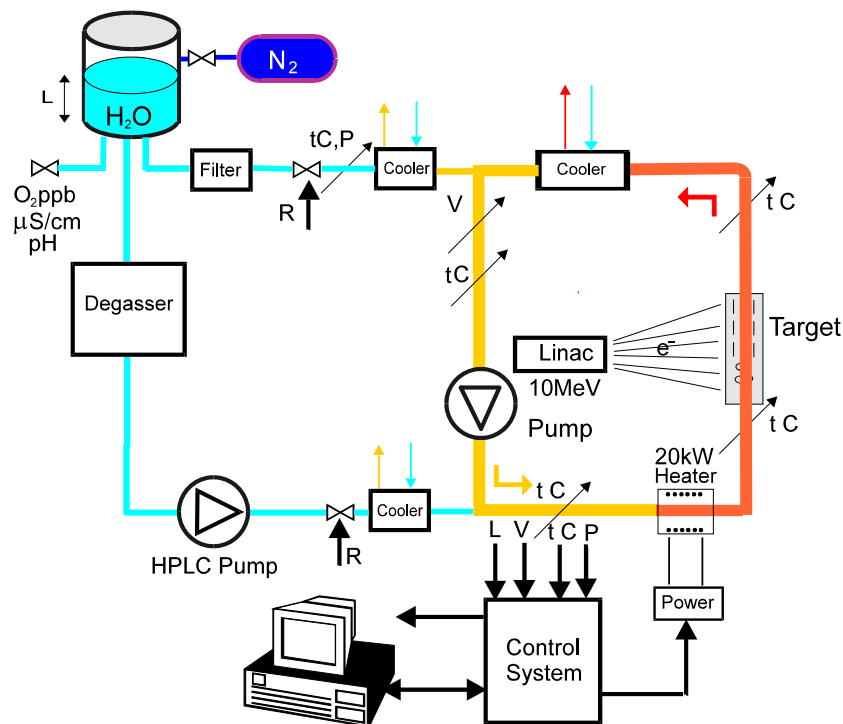


Figure 1 The schematic of the CU-EITF design.

The SCWCL has been designed for a regulated safe operation at temperatures up to 450°C (723 K) and pressures up to 25 MPa. The loop is made of stainless steel 12X18H10T and has an external

pipe diameter 40 mm and wall thickness of 4 mm (different geometries were considered to choose these parameters, see calculation results of section 4). It has two detachable flange connections at the entrances to the irradiation chamber and pump. The water is heated to a temperature above the critical point by the four-section external electric heater with a total capacity of up to 20 kW. Water circulation in the loop is due to natural convection, though it can be adjusted by a 0.5 kW circulation pump. The upper part of the loop is cooled by a tubular cooler.

For chemical analysis and degassing, a small portion of water is discharged from the loop through the capillaries, valves and filter into the accumulation tank partially filled with nitrogen. The recirculation of the water back into the loop after degassing is provided by a high-pressure liquid chromatography pump (HPLC). The operation of automatic valves and pumps is controlled by the Intel™ CPU based PC deployed in-house developed software. For the protection from overheating of the degassing line elements, capillaries are cooled with special coolers to a temperature below 100°C.

The control system is designed to provide routine measurements of pressure, flow rate and temperature at several points on the surface of the loop. The system regulates the supply of electric power in the heaters and controls the operation of pumps and valves. An interlock system incorporates temperature and pressure sensors that can immediately disable heaters, pumps and operation of an accelerator. For extra protection, a mechanical safety valve prevents overpressure above 27 MPa.

The cylindrical irradiation cell (IC) is an integral (but interchangeable) part of the CU-EITF SCWCL. Different ICs can be used in different simulation experiments depending upon the materials under investigation. The reference design is described below, and illustrated in Figure 2.

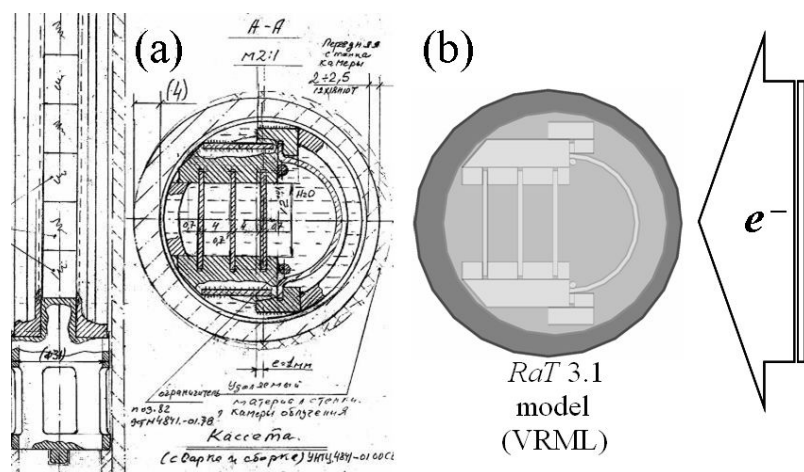


Figure 2 The design drawings (a) and 3D computer model (b) of the CU-EITF irradiation cell.

The irradiation of specimens (as well as additional heating and ionization of the water) occurs in the irradiation cell, exposed to the scanned pulsed electron beam having energy up to 10 MeV, an average beam current up to 1 mA, an electron pulse frequency of 250 Hz, and a scanning frequency of 3 Hz. The longitudinal size of the IC (180 mm) is determined by the linac scanning system amplitude at the front surface of the irradiation chamber. To minimize EB energy losses at the IC front surface, an eccentric design of the IC has been adopted, with a minimum thickness of the front wall of the chamber of 2 mm (see Figure 2(a)).

The arrangement of samples inside the irradiation cell plays a key role in simulation irradiations since it has to provide a predictable variability of material responses to EB energy deposition. For this reason, it is the subject of detailed computer simulation (see section 5). The current IC design (Figure 2) holds a vertically replicated array of groups of four thin specimens having well-defined (by Monte Carlo calculations) positions along the beam propagation line. Three of them are retained in a state free of internal stresses while the front one is arranged to be irradiated in a highly stressed state. In simulation experiments, this opens the possibility of evaluating the combined effects of irradiation and mechanical stresses on the corrosion behaviour and strength of a material.

#### 4. Thermal-hydraulic model of the CU-EITF SCWCL

For assessment of the operational parameters of the circulation loop, a very basic one-dimensional thermal-hydraulic model [11] of single-phase natural convection is currently being applied. However, it can be easily extended to the case of forced circulation, and will be refined at subsequent stages of the Project, taking into account experimental data obtained.

The thermodynamic and kinetic properties of sub- and supercritical water are taken based on the reference IAPWS-97 data [12] available from U.S. National Institute of Standards and Technology databases (<http://webbook.nist.gov/chemistry/fluid>). They are implemented in the calculations by means of a specially developed data acquisition layer in our computer codes.

The variation of single-phase flow parameters (density  $\rho$ , velocity  $v$ , pressure  $p$ , enthalpy  $h$ ) along the path  $x$  of the loop is governed by the balance equations of mass (1.1), momentum (1.2) and energy (1.3) supplemented with the equation of state (1.4):

$$\frac{\partial}{\partial t} \rho + \frac{\partial}{\partial x} (\rho \cdot v) = 0, \quad (1.1)$$

$$\frac{\partial}{\partial t} (\rho \cdot v) + \frac{\partial}{\partial x} (\rho \cdot v^2) + \frac{\partial}{\partial x} p + C_k \cdot \rho \cdot v^2 + \rho \cdot g \cdot \sin \theta = 0, \quad (1.2)$$

$$\frac{\partial}{\partial t} \left[ \rho \cdot \left( h + \frac{v^2}{2} \right) \right] + \frac{\partial}{\partial x} \left[ \rho \cdot v \cdot \left( h + \frac{v^2}{2} \right) \right] + \rho \cdot v \cdot g \cdot \sin \theta = \frac{\partial}{\partial t} p + q, \quad (1.3)$$

$$\rho = \rho(p, h) \quad (1.4)$$

where  $C_k$  accounts for the dynamical friction factor,  $q$  (W/cc) is the specific heating power (assumed to be completely discharged by the loop cooler in a steady-state mode),  $g$  is the gravitational acceleration, and an angle  $\theta$  defines the slope of the loop segment *wrt* the horizontal plane.

It follows from Eq. 1.1 that the mass flow rate  $w = \rho \cdot v$  (kg/s/cm<sup>2</sup>) is conserved for a closed loop in a steady-state mode when  $\partial/\partial t = 0$  in equations (1.1–3). Then the system of balance equations reduces to ordinary differential equations (2):

$$\frac{d}{dx} w = 0, \quad (2.1)$$

$$\frac{d}{dx} \left( \frac{w^2}{\rho} \right) + \frac{d}{dx} p + C_k \cdot \frac{w^2}{\rho} + \rho \cdot g \cdot \sin \theta = 0, \quad (2.2)$$

$$\frac{d}{dx} \left[ w \cdot \left( h + \frac{w^2}{2\rho^2} \right) \right] + w \cdot g \cdot \sin \theta = q. \quad (2.3)$$

The enthalpy profile  $h(x)$  can be evaluated from Eq. 2.3 in the first (linear) approximation as

$$h(x) = h(0) + \frac{q - w \cdot g \cdot \sin \theta}{w} \cdot x + O \left[ \frac{w^2}{2\rho^2(h(x))} - \frac{w^2}{2\rho^2(h(0))} \right]. \quad (3)$$

Then the solution of Eq. 2.2 yields

$$\Delta p(x, w) = p(x, w) - p(0, w) = \frac{w^2}{\rho(h(0))} - \frac{w^2}{\rho(h(x))} - w^2 \int_0^x \frac{C_k(x, w, h(x))}{\rho(h(x))} dx - g \cdot \int_0^x \rho(h(x)) \cdot \sin \theta(x) dx. \quad (4)$$

Equation (4) is easily generalized to the case of forced convection by addition of the term  $\Delta p_p(w)$  specific to the particular circulation pump. For a steady-state operation of a closed loop of length  $L$ , the enthalpy  $h$  is a periodical function of  $x$  ( $h(0) = h(L)$ ), and the overall pressure drop vanishes:

$$\oint_{\text{loop}} \Delta p(x, w) dx = 0. \quad (5)$$

The steady-state mass flow rate  $w$  is a root of Eq. 5. Due to its conservation (Eq. (2.1)),  $w$  determines the profiles of mass  $W = w \cdot S(D)$  and linear  $v = w/r$  velocities in a flow (here  $S$  and  $D$  are the loop pipe cross-section area and hydraulic diameter, respectively). Since the specific heat capacity  $c_p(p, T) = [\partial h(p, T) / \partial T]_p$ , the enthalpy profile of Eq. 3 allows calculation of temperatures in the vicinity of the loop, and particularly of the maximal outlet temperature  $T_{\text{out}}$  based on given inlet temperature  $T_{\text{in}}$ .

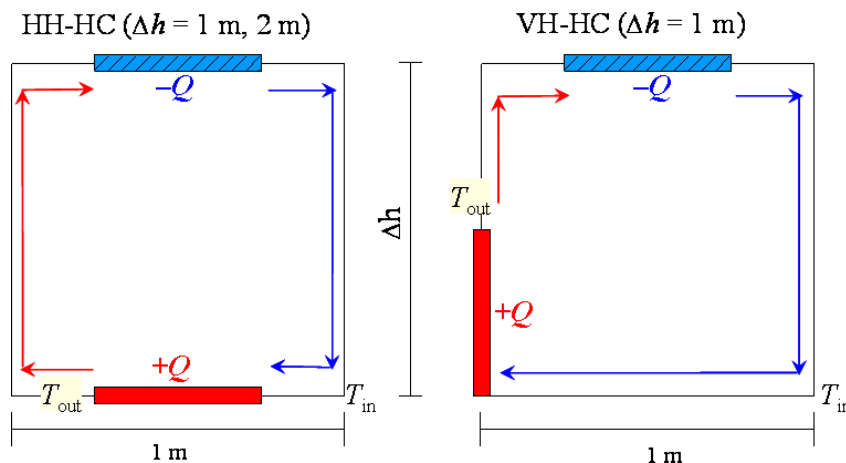


Figure 3 Typical schemes of natural convection loops with horizontal heater and cooler (HH-HC), and vertical heater and horizontal cooler (VH-HC).

A computer code was developed to solve equation (5) for flexible models of circulation loops of segmented structure (see Figure 3): each segment is characterised by the geometrical parameters, applied heating/cooling power density, and friction factors. The following friction model is implemented:

$$C_k(x, w, h) \cdot \Delta x = \frac{f(Re) \cdot \Delta x}{2 \cdot D} + \sum_i K_i \cdot \delta(x - x_i) \cdot \Delta x \quad (6)$$

where  $Re = w \cdot D / \mu(h)$  is the Reynolds number,  $\mu(h)$  is the dynamical viscosity of a fluid,  $f(Re) = \max\left(\frac{64}{Re}, \frac{0.3164}{Re^{0.25}}\right)$  describes dynamical friction in laminar and turbulent flows, and  $K_i$  are (phenomenological) local friction factors of the segments of a convection loop.

Selected results of the CU-EITF type SCWCL characterization within the framework of the described model are shown in Figures 4 and 5. Two major features of these results were taken into account during the design work on the CU-EITF loop: (i) the predicted “saturation” of mass transfer rate effectively restricts the range of required heater power  $Q$  to moderate values of 20–30 kW, and (ii) rapid growth of  $T_{out}$  at high  $Q$ , small  $D$  and/or high local hydraulic resistance  $K$  of component parts can result in the facility overheating. These considerations have stipulated the conservative choice of the piping internal diameter being 32 mm and the heater power being 20 kW.

However, very acceptable mass (~50 g/s) and linear (~1 m/s) rates of SCW natural convection flow are obtainable using these parameters.

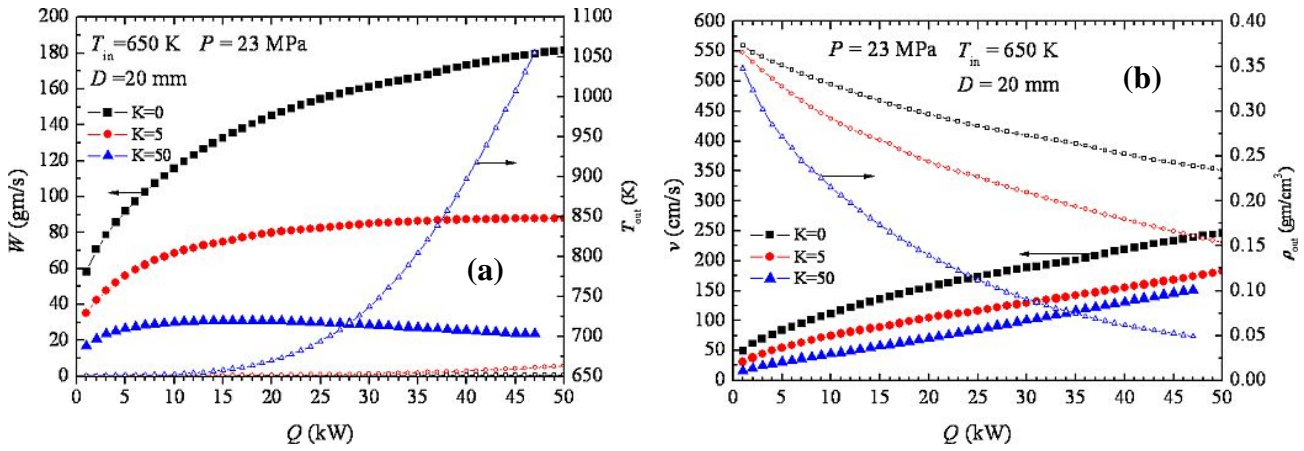


Figure 4 Calculated dependencies of the SCW mass velocity  $W$  and maximal outlet temperature  $T_{out}$  on (a), linear velocity  $v$  and SCW density  $\rho_{out}$  at the heater outlet (b) the SCWCL heater power  $Q$ .

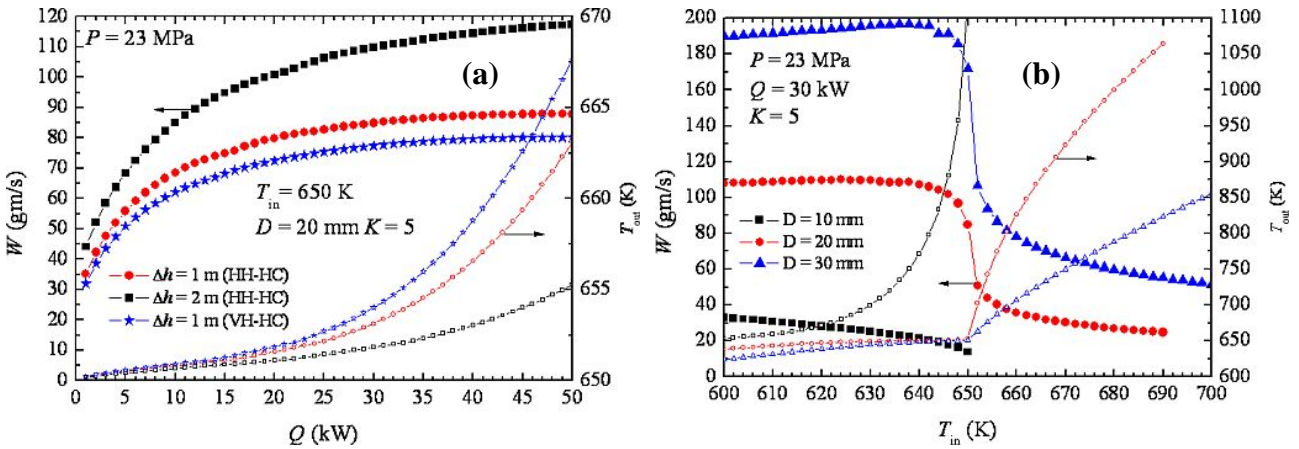


Figure 5  $Q$ -dependencies of  $W$  and  $T_{out}$  for different configurations of SCWCL (a) and the dependencies on the inlet temperature  $T_{in}$  at  $Q = 30$  kW (b).

Further extensions of the SCWCL model and the corresponding computer code are directed toward the capability of numerical solution of time-dependent equations (1) for evaluation of SCW flow instabilities and transient modes of SCWCL operation.

### 5. Monte Carlo simulation of radiation fluxes and EB energy deposition

Alongside common requirements of mechanical strength for high-pressure experimental setups, the decisive arguments for selection of the CU-EITF irradiation chamber design followed from an extensive set of Monte Carlo simulation of the interaction of LPE-10 linac  $e$ -beam with different models of a target assembly containing SCW and models of irradiated specimens.

The in-house developed Monte Carlo radiation transport code RaT 3.1, based on the CERN GEANT4 Object Oriented Toolkit [13] version 4.9.3, has been used for simulation. The GEANT4 capability of consistent statistical modelling of electromagnetic ( $e^\pm, \gamma$ ) and hadronic interaction processes for

complex 3D models of targets provides adequate support of the simulation experiments [6-8], taking into account the problem-oriented extensions implemented in the RaT code. It is a multi-purpose GEANT4 application designed mainly for a wide range of computational dosimetry calculations followed by the estimation of nuclear engineering responses of topical structural materials (energy deposition, point defect production, neutron and gamma activation, *etc.*). To optimize the IC design, the current version 3 of the RaT code had been upgraded to meet the Project requirements of sub-millimeter spatial resolution of the simulation of responses of a complex 3D setup of the IC (see Figure 2) to EB irradiation.

Monte Carlo calculations were carried out for nominal parameters of the CU-EITF *e*-beam: energy 10 MeV, electric power 7 kW, EB current density  $9.7 \mu\text{A}/\text{cm}^2$ , beam scan area  $40 \times 180 \text{ mm}$ . It was assumed that the IC is filled with model 0.7 mm thick SS samples. Water filling of the IC was modelled at three characteristic densities  $\rho = 0.3, 0.6, \text{ and } 1.0 \text{ g}/\text{cm}^3$ . Different versions of IC geometry were simulated to find the optimal one. Only the final results of these studies are discussed below.

2D colour maps of radiation flux distributions in the irradiation chamber at  $\rho = 0.3 \text{ g}/\text{cm}^3$  are shown in Figure 6. It is clearly seen that the IC completely absorbs primary electrons while converting their energy into significant fluxes of  $\gamma$ -quanta and secondary electrons. This means that the IC design is optimized with respect to the total utilization of the LPE-10 linac EB power.

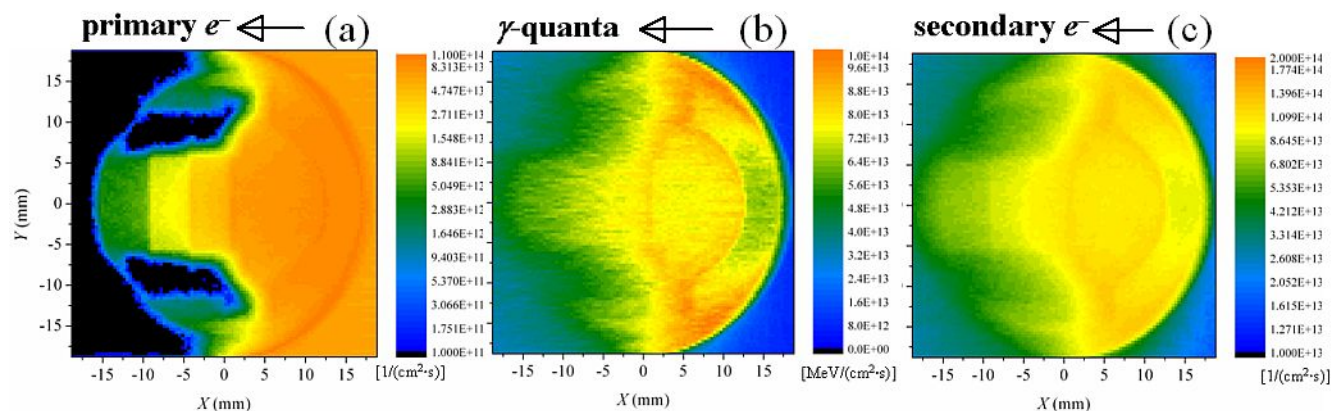


Figure 6 2D spatial distributions of axially averaged fluxes of primary electrons (a), bremsstrahlung gamma quanta (b) and secondary (mainly Compton) electrons (c) inside the IC of Figure 2.

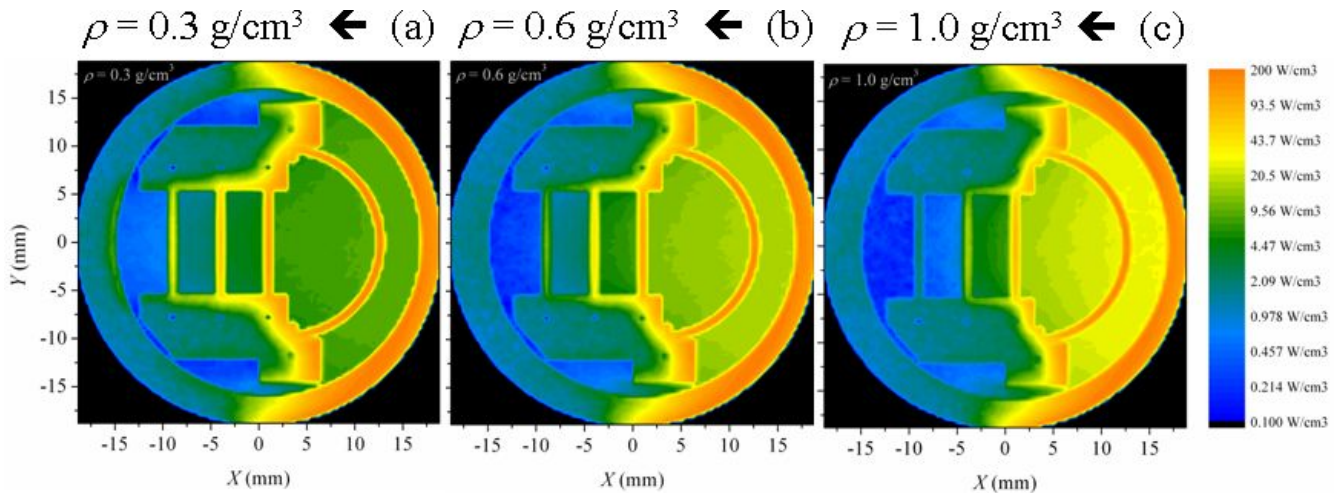


Figure 7 2D spatial distributions of axially averaged specific EB power deposition in the CU-EITF irradiation cell at various densities  $\rho$  of water flow.

Similar distributions have been obtained for the specific power deposition ( $\text{W}/\text{cm}^3$ ) inside the IC (see Figure 7). They show a clear correlation with the IC geometry depicted in Figure 2.

However, of greater importance is the quantitative representation of data in Figure 8. The depth profiles show that the energy deposition is essentially inhomogeneous. The irradiation load of samples varies considerably along the beam penetration path, especially at higher densities of water flow. This suggests that the simulation experiments will be able to clarify dose dependencies of corrosion of relevant materials in the SCW coolant.

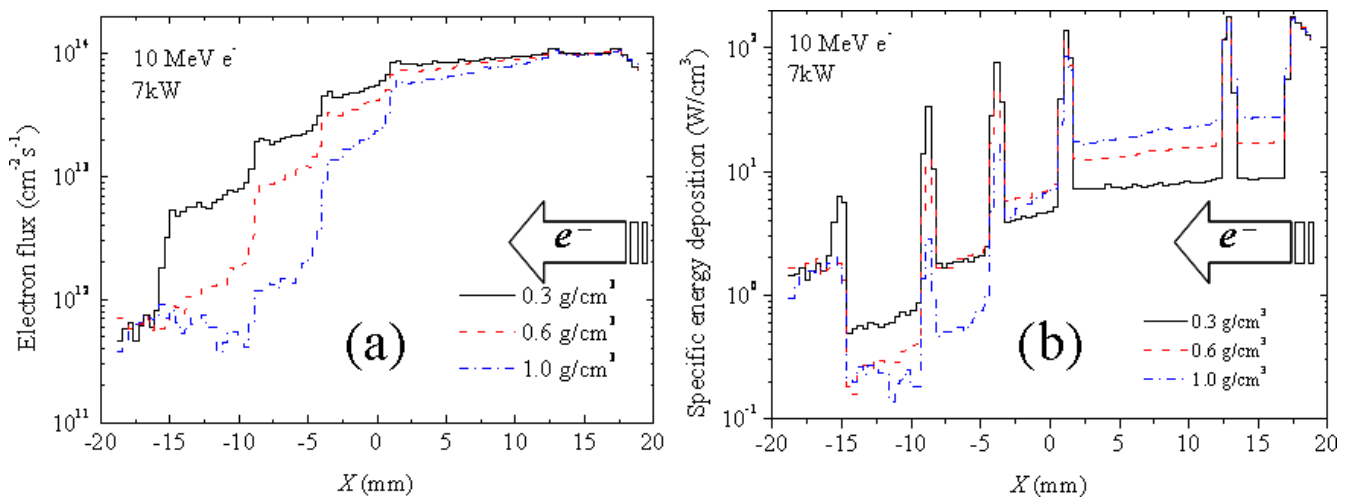


Figure 8 The  $e^-$ -beam penetration depth dependencies of total electron flux (a) and specific deposited power at the midplane in the CU-EITF IC at various densities  $\rho$  of water flow.

## 6. FEM analysis of temperature fields inside the irradiation cell

Temperature fields in the SCWCL IC are determined by the  $e$ -beam deposited power distribution and by the heat transfer between different component parts of IC (*incl.* SCW flow) and environment. Figure 8(b) clearly shows that the specific power deposition  $P_{\text{SCW}}$  in the SCW is much smaller than that in the metal parts of the IC. Obviously, this is due to the much smaller density and effective atomic number of coolant. At high flow rates ( $W = 50$  g/s) the SCW is heated by the  $e$ -beam during a rather short time  $\Delta t \approx \rho V/W$ , where  $\rho V$  is the mass of SCW in the IC of free volume  $V$ . The increase  $\Delta T$  of the SCW temperature induced by immediate deposition of EB power can be estimated disregarding heat transfer between coolant and IC walls and specimens:  $\Delta T = P_{\text{SCW}}/[W \cdot c_p(p_0, T_0)]$ , where  $c_p(p_0, T_0)$  is the specific heat capacity of SCW calculated for constant pressure  $p_0$  and temperature  $T_0$  at the IC entrance. These simple calculations argue that  $\Delta T$  is marginal ( $< 0.1$  K) at  $T_0 = 650$  K and  $p_0 = 23$  MPa. Moreover, an upper bound of  $\Delta T$  at conservative assumption of  $P_{\text{SCW}} = P_{\text{beam}} = 7$  kW does not exceed  $\sim 1$  K. This means that the contribution of  $e$ -beam to the heating of the SCW flow is small under the operating conditions of the SCWCL, and the major impact of EB irradiation on the flowing SCW is expected to be due to ionization and radiolysis.

On the other hand, the EB impact on the thermal mode of the fixed parts of the IC can be rather significant, and has to be predicted since the temperature of the irradiated samples is an essential parameter of the simulation experiments. This task has been accomplished using Finite Elements Method (FEM) calculations of 2D stationary temperature distributions  $T(\mathbf{r})$ ,  $\mathbf{r} = (x, y)$ , in the IC.

Inside the disconnected region  $\Omega$  of the IC component parts and samples,  $T(\mathbf{r})$  obeys the heat equation  $\nabla(\kappa(\mathbf{r})\nabla T) = Q(\mathbf{r})$ ,  $\mathbf{r} \in \Omega$ , where  $\kappa(\mathbf{r})$  is the thermal conductivity coefficient of the IC structural material. This partial differential equation is supplemented with the Newtonian boundary condition  $\kappa(\mathbf{r})\frac{\partial T}{\partial \mathbf{n}}\Big|_{\Gamma_{\text{in}}} = \lambda \cdot (T - T_0)$ ,  $\mathbf{r} \in \Gamma_{\text{in}}$ , at internal interfaces  $\Gamma_{\text{in}}$  with the SCW coolant, and the radiative one  $\kappa(\mathbf{r})\frac{\partial T}{\partial \mathbf{n}}\Big|_{\Gamma_{\text{out}}} = \sigma \cdot (T^4 - T_\infty^4)$ ,  $\mathbf{r} \in \Gamma_{\text{out}}$ ,  $\sigma = 5.67 \cdot 10^{-8} \text{ W} \cdot \text{m}^{-2} \cdot \text{K}^{-4}$ , at the outer wall  $\Gamma_{\text{out}}$  of the IC. The heat transfer coefficient  $\lambda = Nu \cdot \kappa_{\text{SCW}}(p_0, T_0)/D$  was calculated using the Dittus-Boelter correlation for Nusselt number  $Nu = 0.023 \cdot Re^{0.8} \cdot Pr^{0.4}$  where  $Pr = \nu_{\text{SCW}}/\kappa_{\text{SCW}}$  is the Prandtl number of SCW, and  $\nu_{\text{SCW}}$  and  $\kappa_{\text{SCW}}$  are kinematical viscosity and thermal conductivity of coolant, respectively. To solve the boundary problem, the package FreeFEM++ 3.9 [14] was applied. The heat source term  $Q(\mathbf{r})$  was taken from the RaT 3.1 Monte Carlo code calculated database of specific power deposition (see Figure 7) mapped onto the FEM mesh model of the irradiation chamber (see Figure 9).

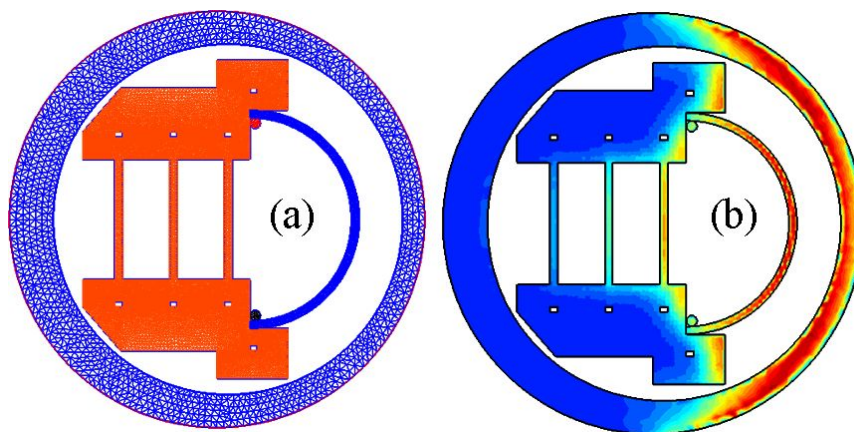
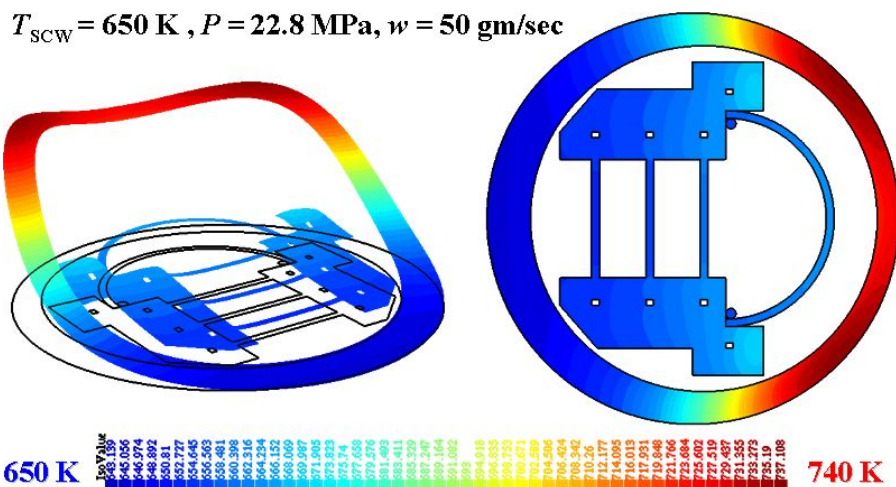


Figure 9 FEM model of the CU-EITF IC (a) associated with the RaT Monte Carlo code calculated 2D spatial distribution of  $e$ -beam specific energy deposition  $Q(\mathbf{r})$  (b).

The results of the temperature field calculations at an SCW temperature of  $T_0 = 650$  K and ambient temperature  $T_\infty = 300$  K are depicted in Figure 10. One can see that the only region where significant (up to +90 K)  $e$ -beam heating occurs is the front wall of the IC. Therefore, the temperature gradient induced thermoelastic stress has to be calculated, and possible supplementary outer cooling of the IC has to be implemented to prevent an increase of the temperature above the CU-EITF projected limit (720 K).



cells makes the proposed methodology of simulation experiments a very efficient tool to supplement the data needed to qualify in-core materials for the SCWR.

This work was supported by the Science & Technology Center in Ukraine under the STCU Project No. P4841.

## 8. References

- [1] U.S. DOE nuclear energy research advisory committee and the Generation IV international forum, “A Technology Roadmap for Generation IV Nuclear Energy Systems”, GIF-002-00, (December 2002).
- [2] R.B. Duffey, H.F. Khartabil, I.L. Pioro, J.M. Hopwood, “The future of nuclear: SCWR Generation IV high performance channels”, Proc. of the 11<sup>th</sup> Int. Conf. on Nuclear Engineering (ICONE-11), Shinjuku, Tokyo, Japan, April 20–23, 2003, Paper No. 36222, 8 pages.
- [3] G.S. Was, P. Ampornrat, G. Gupta, S. Teysseyre, E.A. West, T.R. Allen, K. Sridharan, L. Tan, Y. Chen, X. Ren, C. Pister, “Corrosion and stress corrosion cracking in supercritical water”, *Journal of Nuclear Materials*, Vol. 371, 2007, pp. 176–201.
- [4] A.N. Dovbnya, N.I. Aizatsky, Ye.Z. Biller, V.N. Boriskin, V.A. Kushnir, V.V. Mitrochenko, V.A. Popenko, Yu.D. Tur, V.L. Uvarov, E.S. Zlunitsyn, A.I. Zykov, “Electron Linacs Based Radiation Facilities of Ukrainian National Science Centre KIPT”, *Bulletin of the American Physical Society*, Vol. 42, Iss. 3, 1997, p. 1391.
- [5] M.I. Ayzatsky, V.N. Boriskin, A.M. Dovbnya, V.A. Kushnir, V.A. Popenko, V.A. Shendrik, Yu.D. Tur, A.I. Zykov, “The NSC KIPT Electron Linacs R&D”, *Problems of Atomic Science and Technology. Ser.: Nuclear Physics Investigations*, Iss. 2(41), 2003, pp. 19-24.
- [6] “Materials for molten salt reactors”, Guest eds. A.S. Bakai and F.A. Garner, *Problems of Atomic Science and Technology. Ser.: Radiation Damage Physics and Radiation Materials Science*, Iss. 4(87), 2005, entire issue available online at <http://vant.kipt.kharkov.ua>.
- [7] A.S. Bakai, “Combined effect of molten fluoride salt and irradiation on Ni-based alloys”, Proc. of the NATO Advanced Study Institute on Materials Issues for Generation IV Systems: Status, Open Questions and Challenges. Cargese, Corsica, France, Sept. 24 – Oct. 6 2007, Springer Netherlands, 2008, XV, pp. 537–557.
- [8] A.S. Bakai, S.V. Dyuldya, “Construction materials for molten salt reactor: design and tests under  $e$ -irradiation”, Book of extended synopses of Int. Conf. on Fast Reactors and Related Fuel Cycles — Challenges and Opportunities (FR09), Dec. 7–11, 2009, Kioto, Japan, p. 417.
- [9] M.H. Anderson, J.R. Licht, M.L. Corradini, “Progress on the University of Wisconsin supercritical water heat transfer facility”. Proc. of the 11<sup>th</sup> Int. Topical on Nuclear Reactor Thermal-Hydraulics (NURETH 11), Avignon, France, October. 2–6, 2005, paper 265.
- [10] S. Teysseyre, Q. Peng, C. Becker, G.S. Was, “Facility for stress corrosion cracking of irradiated specimens in supercritical water”, *Journal of Nuclear Materials*, Vol. 371, 2007, pp. 98–106.

- [11] M. Sharma, D.S. Pilkhwal, P.K. Vijayan, D. Saha, R.K. Sinha, “Steady state and linear stability analysis of a supercritical water natural circulation loop”, *Nuclear Engineering and Design*, Vol. 240, 2010, pp. 588–597.
- [12] W. Wagner, J.R. Cooper, A. Dittmann, “The IAPWS formulation 1997 for the thermodynamic properties of water and steam”, *J. Eng. Gas Turbines Power*, Vol. 122, 2000, pp. 150-182.
- [13] S. Agostinelli, J. Allison, A. Forti, N. Savvas, J. Apostolakis, P. Arce, H. Burkhardt, R. Chytracsek, G. Cosmo, G. Folger, S. Giani, V. Ivanchenko, V. Lara, M. Liendl, E. Medernach, A. Pfeiffer, S. Sadilov, H. Araujo, A. Howard, S. Banerjee, et al., “GEANT4 — a simulation toolkit”, *Nuclear Instruments and Methods. Sec. A*, Vol. 22, Iss. 3, 2003, pp. 250–303.
- [14] <http://www.freefem.org/ff++>.